Commissioning of the tongue-and-groove modelling in treatment planning systems: from static fields to VMAT treatments

Commissioning of the tongue-and-groove modelling in treatment planning systems: from static fields to VMAT treatments

Victor Hernandez†¶, Juan Antonio Vera-Sánchez†, Laure Vieillevigne‡ and Jordi Saez§

† Department of Medical Physics, Hospital Universitari Sant Joan de Reus, IISPV, 43204 Tarragona, Spain

‡ Department of Medical Physics, Institut Claudius Regaud - Institut Universitaire du Cancer de Toulouse, 31059 Toulouse, France

§ Department of Radiation Oncology, Hospital Clínic de Barcelona, 08036 Barcelona, Spain

Abstract. Adequate modelling of the multi-leaf collimator (MLC) by treatment planning systems (TPS) is essential for accurate dose calculations in intensity-modulated radiation-therapy. For this reason modern TPSs incorporate MLC characteristics such as the leaf end curvature, MLC transmission and the tongue-and-groove. However, the modelling of the tongue-and-groove is often neglected during TPS commissioning and it is not known how accurate it is. This study evaluates the dosimetric consequences of the tongue-and-groove effect for two different MLC models using both film dosimetry and ionisation chambers. A set of comprehensive tests are presented that evaluate the ability of TPSs to accurately model this effect in (a) static fields, (b) sliding window beams and (c) VMAT arcs. The tests proposed are useful for the commissioning of TPSs and for the validation of major upgrades. With the ECLIPSE TPS, relevant differences were found between calculations and measurements for beams with dynamic MLCs in the presence of the TG effect, especially for the High Definition MLC, small gap sizes and the 1 mm calculation grid. For this combination, dose differences as high as 7% and 10% were obtained for dynamic MLC gaps of 5 mm and 10 mm, respectively. These differences indicate inadequate modelling of the tongue-and-groove effect, which might not be identified without the proposed tests. In particular, the TPS tended to underestimate the calculated dose, which may require tuning of other configuration parameters in the TPS (such as the dosimetric leaf gap) in order to maximise the agreement between calculations and measurements in clinical plans. In conclusion, a need for better modelling of the MLC by TPSs is demonstrated, one of the relevant aspects being the tongue-and-groove effect. This would improve the accuracy of TPS calculations, especially for plans using small MLC gaps, such as plans with small target volumes or high complexities. Improved modelling of the MLC would also reduce the need for tuning parameters in the TPS, facilitating a more comprehensive configuration and commissioning of TPSs.
(Some figures appear in colour only in the online journal)

¶ To whom correspondence should be addressed (vhernandezmasgrau@gmail.com)

Commissioning of the tongue-and-groove modelling in TPS 2

1. Introduction

It is well known that adequate modelling of the multi-leaf collimator (MLC) is essential for accurate dose calculations in intensity-modulated radiation-therapy (IMRT) treatments involving dynamic MLCs (Lorenz et al.; 2008; Li et al.; 2010). For this reason, modern treatment planning systems (TPSs) incorporate MLC characteristics such as the leaf end curvature, MLC transmission and the tongue-and-groove.

Transmission through the MLC is defined as a ratio between the doses from an open field and a field with a fully closed MLC. Transmission between leaves (interleaf transmission) is higher than the average transmission due to the thin layer of air between leaves, which reduces the ability of the MLC to shield the beam. Therefore, many MLC models have a 'tongue-and-groove' design, where the sides of adjacent leaves interlock in order to minimise interleaf transmission. However, this arrangement can produce underdosage between adjacent leaf pairs in asynchronous MLC movements due to this region being further shielded by the tongue of opposing leaf sides in different phases of treatment delivery (Deng et al.; 2001). This underdosage is known as the tongue-and-groove effect (TG effect).

In general, IMRT plans may involve many highly irregular and small MLC apertures and in volumetric-modulated arc therapy (VMAT) individual leaves may repeatedly extend into the radiation field, giving rise to considerable TG effects. Proper modelling of all MLC characteristics is particularly relevant, therefore, in VMAT treatments (Mans et al.; 2016). Nevertheless, it is difficult for a TPS to fully consider the effects of the beam delivery system (Li et al.; 2010). Some investigators (Van Esch et al.; 2011) have reported that TPS calculations are able to reproduce patterns of dose dips and peaks for a static test field with maximum TG effect. However, the accuracy of the tongue-and-groove modelling in treatments with dynamic MLCs has not been thoroughly investigated.

Since the modelling of tongue-and-groove, rounding of the leaf tips and MLC transmission is essential, these aspects must be considered in the TPS commissioning. Despite that, current guidelines do not include specific tests for the tongue-and-groove, which is often neglected during TPS commissioning (IAEA; 2007, 2008; Smilowitz et al.; 2015; Mans et al.; 2016).

The purpose of this study is to evaluate the modelling of the TG effect in TPSs and to provide comprehensible procedures for the commissioning of TPSs regarding this effect. To this aim, the TG effect is characterised and calculations are compared to measurements for (1) static fields, (2) sliding window beams and (3) VMAT arcs. In particular, a novel test that allows a simple and practical evaluation of both the impact of the TG effect in VMAT treatments and the accuracy of TPS calculations is presented.

Commissioning of the tongue-and-groove modelling in TPS　　　　　　3

2. Materials and Methods

This study focuses on the ECLIPSE TPS and Varian linear accelerators. In the subsequent sections we describe the equipment (section 2.1), tests (section 2.2) and measurements (section 2.3) used.

2.1. Equipment

Three institutions participated in the study and measurements from four linear accelerators (linacs) were evaluated. The study was mainly conducted in centre A, with 2 linear accelerators: a Varian Trilogy^{TM} equipped with a high definition MLC (HDMLC) and an iX linac with a Millennium120 MLC. For comparison purposes, several tests were repeated for two more linacs from different institutions: a TrueBeam STx system equipped with an HDMLC (centre B) and a 2100CD linac with a Millennium120 MLC (centre C). All experiments were carried out with X-rays with a nominal energy of 6 MV.

The HDMLC consists of 60 pairs of leaves: 32 inner leaves of 2.5 mm width and 28 outer leaves with a leaf width of 5.0 mm defined at the isocentre plane. The Millennium120 MLC also consists of 60 pairs of leaves: 40 inner leaf pairs 5 mm wide and 20 outer leaf pairs of leaves that are 10 mm wide at the isocentre plane. Thus, the maximum field length in the in-plane direction is 22 cm for the HDMLC and 40 cm for the Millennium120 MLC. There are important differences between these two MLC models, such as leaf height, leaf tip curvature and material composition. Detailed information on their exact geometry and characteristics can be found in the literature (Fix et al.; 2011). For both models the extensions of the tongue (protruding part of half the leaf edge that sticks out into the adjacent leaf) and the groove (stretching of the other half of the leaf edge) are 0.4 mm.

Different versions of the ECLIPSE TPS were evaluated: v13 (centre A), v11 and v13 (centre B) and v10 (centre C). The Analytical Anisotropic Algorithm (AAA) was used, which is an analytical photon dose calculation algorithm based on pencil beam convolution/superposition methods. VMAT plans were also calculated with AcurosXB, which belongs to the class of the Linear Boltzmann Transport Equation solvers and calculations were renormalised to the corresponding $10 \times 10\,cm^2$ field to minimise differences between algorithms. All calculations were carried out with two calculation grid sizes: 2.5 mm and 1 mm. The 2.5 mm grid was selected because it is commonly used in clinical practice. The grid of 1 mm was evaluated because it is the finest resolution allowed by the TPS and assessing the fine details of the tongue-and-groove structure prompts the use of the smallest available grid size.

The linacs, MLCs, TPSs and calculation algorithms investigated in this study are summarised in table 1. All TPSs were commissioned according to international protocols.

Commissioning of the tongue-and-groove modelling in TPS 4

Table 1. Summary of the equipment used

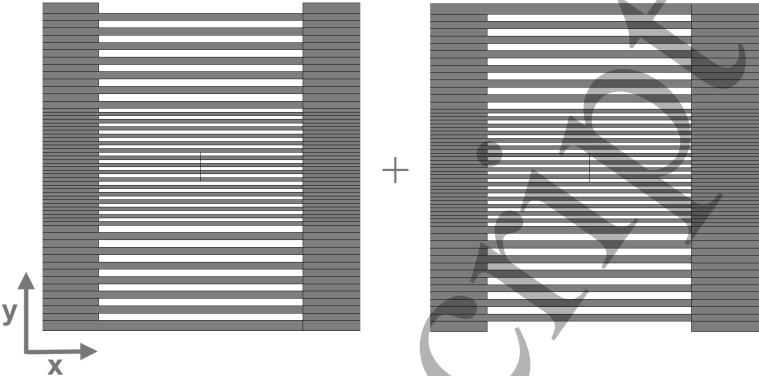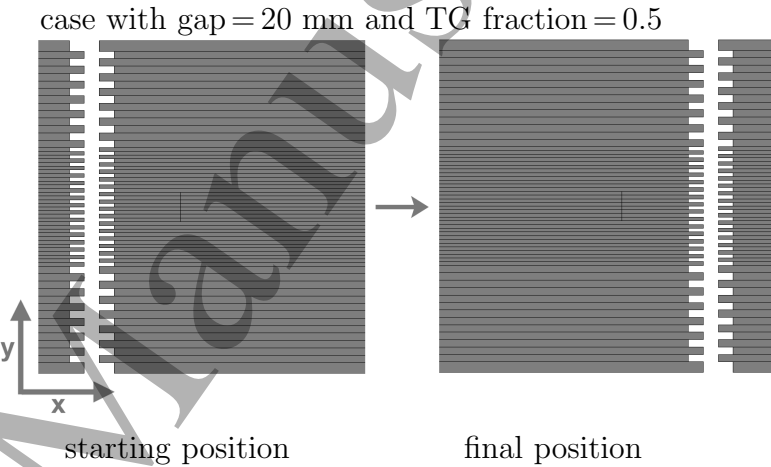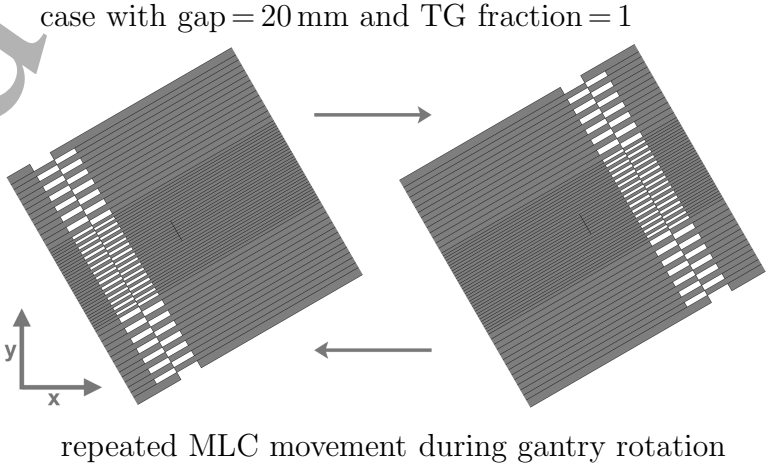| Centre	Linac	MLC model	TPS	Calculation algorithms
A	Trilogy$^{\text{TM}}$	HDMLC	Eclipse 13.5.35	AAA & AcurosXB
A	2300iX	Millennium120	Eclipse 13.5.35	AAA & AcurosXB
B	TrueBeam STx	HDMLC	Eclipse 11.0.31 & 13.7.14	AAA
C	2100CD	Millennium120	Eclipse 10.0.28	AAA

2.2. Tests

Three types of tests were devised, involving (1) static fields, (2) sliding window beams and (3) VMAT arcs. The main characteristics of the tests are given in the following subsections and sketched in table 2. All DICOM plan files corresponding to these tests will be provided by the authors upon request.

2.2.1. Static fields

A combination of two static fields was used to evaluate the case with maximum TG effect. The first field was defined by an MLC where all leaves with even numbers were open while their neighbour leaves (with odd numbers) were closed. The second field consisted of the complementary MLC, with even leaves closed and odd leaves open. Field jaws were set to $12 \times 22 \, \text{cm}^2$ and $12 \times 32 \, \text{cm}^2$ for fields with the HDMLC and the Millennium MLC, respectively, in order to include information from leaves of different widths.

Similar MLC patterns have been used in the literature (Van Esch et al.; 2011; Fix et al.; 2011). The interest of this test is that the combination of the two static fields generates a uniform dose distribution except for the TG effect. As a consequence, a clear pattern is produced with underdosage at the positions corresponding to leaf edges. Thus, this test provides information about the dosimetric consequences of the maximum TG effect caused by the different leaves.

2.2.2. Sliding window beams

The sliding window technique involves beams with static gantry and dynamic MLCs. The MLC leaves start at one side of the field and move unidirectionally towards the opposite side while the beam is on. A typical test involving dynamic MLCs is the sweeping gap test, where all leaves are uniformly extended defining a certain gap and move at the same constant speed (LoSasso et al.; 1998).

Since the sweeping gap test involves uniformly extended leaves, it does not generate any TG effect. To incorporate the TG effect, a shift was applied to the position of adjacent leaves, generating a 'moving fence pattern'. Thus, all leaves with even number were shifted with respect to their neighbour leaves, generating a fence-shaped MLC pattern (as illustrated in table 2). Despite the shift, all leaves moved at the same constant speed, keeping the MLC pattern unchanged. The same gap size was produced by all leaf pairs, but, since leaves are not uniformly extended, this test incorporated a

Commissioning of the tongue-and-groove modelling in TPS   5

Tests	MLC
(a) Static test – static gantry – sum of two static MLCs gantry $= 0°$ collimator angle $= 0°$ X $= 10$ cm Y $= \begin{cases} 22 \text{ cm (HDMLC)} \\ 32 \text{ cm (Millennium)} \end{cases}$	
(b) Asynchronous sweeping gap test (a-SG) – static gantry – dynamic MLC gantry $= 0°$ collimator angle $= 0°$ X $= 10$ cm Y $= \begin{cases} 22 \text{ cm (HDMLC)} \\ 32 \text{ cm (Millennium)} \end{cases}$ gaps $= 5, 10, 20, 30$ mm several TG fractions	case with gap $= 20$ mm and TG fraction $= 0.5$ starting position final position
(c) Asynchronous oscillating sweeping gap test (a-OSG) – VMAT arc – dynamic MLC gantry $=$ Full rotation collimator angle $= 30°$ X $= 6$ cm Y $= 8$ cm gaps $= 10, 20, 30$ mm several TG fractions	case with gap $= 20$ mm and TG fraction $= 1$ repeated MLC movement during gantry rotation

Table 2. Tests used for (a) static fields, (b) sliding window beams and (c) VMAT arcs. The main settings and a sketch of the MLCs used for each test is provided

Commissioning of the tongue-and-groove modelling in TPS 6

certain degree of TG effect that depends on the value of the shift. Similar tests have been used by other investigators (Rosca and Zygmanski; 2008; Yao and Farr; 2015). In the present study this test will be referred to as the asynchronous sweeping gap (a-SG) test.

The files for the a-SG test were created by modifying the DICOM files provided by the manufacturer for the sweeping gap test, where the centre of the MLC gap moves from -6 cm to +6 cm with 13 control points that define the position of the leaves every 10 mm to ensure that the off-axis correction for the MLC is accurately applied (Mei et al.; 2011). The field size was the same as used for the static field test and the collimator rotation was kept at 0°. The investigated MLC gap widths were 5, 10, 20 and 30 mm in order to include the range of gaps representative of clinical treatments. For each gap width g, a range of shifts s were evaluated and the tongue-and-groove fraction was expressed as TG fraction $= s/g$. Thus, for TG fraction $= 0$, all leaves are uniformly distributed and there is no TG effect and the higher the TG fraction, the more important the TG effect. The maximum TG fraction varied between 1 and 2 depending on the gap size due to limitations related to the maximum leaf span of the MLC.

2.2.3. VMAT arcs To investigate the TG effect in VMAT treatments we designed a test based on the oscillating sweeping gap (OSG) test presented by Bhagwat et al. (2010). In the OSG test a uniform MLC gap repeatedly moves across the field at a constant speed during a full gantry rotation. Thus, an approximately uniform dose distribution in a cylindrical volume is created, which allows a simple detection of errors in dose calculations. For this reason, the verification of the MLC beam model inside the TPS is one of the potential applications of the test (Bhagwat et al.; 2010). To this aim, we incorporated the TG effect into the OSG test by introducing a shift between the positions of adjacent leaf pairs as described in the previous section for the a-SG test. This extension of the OSG test will be referred to as the asynchronous oscillating sweeping gap (a-OSG) test.

DICOM plans for this test were generated with an in-house software developed in MATLAB (Mathworks, Massachusetts, USA). Each plan consists of an arc with a gantry rotation between 179° and 181° defined by 178 control points, similar to full arcs from clinical plans. The MLC forms a moving fence pattern that subsequently moves forward and backwards across the field. In particular, the MLC carries out 11 cycles during the gantry rotation from -4.5 cm to +4.5 cm: 6 sweeps in one direction and 5 sweeps in the opposite direction. This code produces VMAT plans where both the gap size and the TG fraction (as defined in the previous section) are selected. The gap sizes investigated were 10 mm, 20 mm and 30 mm and several TG fractions were evaluated for each gap.

All VMAT arcs delivered 700 MU with the maximum dose rate set to 600 MU/min. The same plans (adapted to each MLC model) were used for all linacs, but the resulting dose rate and gantry speed at each control point depended on the maximum gantry speed of the treatment unit. For C-Series linacs (centres A and C) the gantry moved at its maximum gantry speed of 4.8 deg/s and the dose rate was kept around 560 MU/min.

Commissioning of the tongue-and-groove modelling in TPS   7

For the TrueBeam system (centre B), configured with a maximum gantry speed of
6 deg/s, the dose rate was fixed at 600 MU/min and the gantry speed remained at about
5.1 deg/s. In all cases the leaves moved at a constant speed of 1.8 cm/s or 1.9 cm/s,
depending on the treatment unit. The X jaws were set to 6 cm in order to have the
asynchronous MLC gaps completely covering the irradiated volume. The Y jaws were
set to 8 cm, including the contribution only from the central thinner leaves. Similarly
to clinical arcs, the collimator angle was set to 30°, which spatially distributed the TG
effect and the impact of the interleaf transmission.

After creating the DICOM plans, they were imported into the TPS for subsequent
calculation and delivery. The treatment couch was included in TPS calculations as
a support structure for all plans. Having the collimator rotated during the gantry
rotation changes the shape of the volume being uniformly irradiated, which is no longer
cylindrical. Indeed, the quasi-uniform dose volume is circular in axial planes, but the
radius of this circle diminishes as the axial plane moves away from the isocentre. Thus,
an approximately uniform dose distribution is produced with a rhomboid shape in
coronal and sagittal planes, which also allows for simple dose measurements.

2.3. Measurements and TPS configuration

Both film and chamber measurements – once corrected by daily linac output – were
compared to calculations from the TPS. Calculated profiles were compared to those
obtained with film dosimetry as described in the next subsection. Calculated average
doses were also compared to both chamber measurements and average film doses.

2.3.1. Film dosimetry The dose distributions corresponding to static and a-SG tests
were measured using a slabbed RW3 phantom placed at a source-to-surface distance
of 90 cm. Films were positioned horizontally at 10 cm depth with 10 cm slabs for
backscatter. Measurements were also carried out at 2 cm depth for comparison purposes.
The number of MUs was selected to deliver a minimum dose of 80 cGy to the film.

For the a-OSG tests measurements were performed with films placed in the
MultiPlug™ insert of ArcCHECK™ (Sun Nuclear Corp., Melbourne, 225 FL). This is
a polymethyl methacrylate (PMMA) cylindrical phantom with a diameter of 15 cm that
allows measurement with both film and ionisation chamber. Two slabs of low density
polyethylene were cut and used to sustain the MultiPlug™ on the treatment couch by
its borders. The centre of the MultiPlug™ was placed at the isocentre, with a source-
to-surface distance of 92.5 cm and films were placed in a horizontal plane at the isocentre
level. To evaluate the feasibility of using other phantoms for this test, calculations and
measurements were repeated using the cubic EASY CUBE phantom (Euromechanics,
Schwarzenbruck, Germany).

Radiochromic EBT3 films (ISP, Wayne, NJ) were used. For every film, three
pieces of $20.4 \times 3 \, cm^2$ were cut and exposed to known doses in order to perform a three
point re-calibration as described by Lewis et al. (2012). Films were scanned using

Commissioning of the tongue-and-groove modelling in TPS 8

an Epson 10000XL scanner (Seiko EPSON Corp., Nagano, Japan) at least four hours post-exposure. All the pieces from the same film were aligned to the centre of the digitizer bed in portrait orientation and fixed by a 3 mm-thick sheet of glass. Images were acquired using a 150 dpi resolution in RGB mode with 16 bits per channel and with no colour adjustment and were saved in tiff format. An accurate scanning protocol was followed: firstly the scanner was switched on 30 minutes before use; secondly, a warm up of seven open scans was carried out; and finally, 15 images of every film with the same frame were acquired leaving two minutes between consecutive scans. All images from the same film were averaged in order to remove temporal noise and dose maps were obtained from the average images with multichannel dosimetry following the efficient protocol by Lewis et al. (2012). This method provides noise reduction without losing accuracy, as described in a recent work by Vera Sanchez et al. (2016) and it is recommended when a high resolution is desired.

Finally, in-plane profiles were extracted from the dose maps and mean doses in the central $2 \times 2 \text{cm}^2$ region of interest were obtained. Profiles from the static and the a-SG tests were averaged in the cross-plane direction over a region of 1 cm in order to achieve a higher noise reduction by taking advantage of the symmetry of the dose distribution in that direction. To avoid spatial distortion, no filter was applied to images or dose maps; only time averaging (multiple scans) and spatial averaging along the cross-plane direction were considered as de-noising techniques.

2.3.2. Ionisation chamber Dose measurements were carried out using a Farmer-type ionisation chamber positioned at the isocentre along the Y axis, that is, perpendicular to the MLC movement direction with the collimator angle set to 0°. The PTW chamber model 30013 was used, with an active length of 23 mm and an active volume of 0.6 cm^3. This chamber was selected because its active length spanned several leaves, providing an estimate of the average impact of the TG effect.

The static and a-SG tests were measured at 10 cm depth in a (1) water phantom and (2) RW3 plastic phantom for comparison with TPS calculations and film measurements, respectively. Measurements for VMAT (a-OSG test) were performed using the Farmer chamber placed at the centre of the cylindrical PMMA phantom described in the previous section. Chamber readings were corrected for the daily output variations of the linacs and differences between TPS calculations and measurements were calculated as $(D_{\text{TPS}} - D_{\text{measured}})/D_{\text{measured}}$.

2.3.3. MLC modelling and configuration in the ECLIPSE TPS Two user-definable parameters are required during commissioning of the ECLIPSE TPS: the MLC transmission and the dosimetric leaf gap. The TPS uses a single value for transmission that is determined as the ratio of the measured average dose in an open field and the measured average dose for the same field size with the MLC closed. Thus, the TPS considers only the average transmission, without taking into account the higher interleaf transmission, modifications in the energy spectrum of the beam or any variation between

leaves of different width.

The dosimetric leaf gap parameter is used by ECLIPSE to model the higher transmission through the rounded leaves of the MLC. To this aim, the actual fluence used for dose calculations is computed considering a shift in the leaf positions. In particular, leaves are pulled back by half the value of the dosimetric leaf gap, so that the gap between a fully closed leaf pair equals the dosimetric leaf gap parameter.

The tongue-and-groove is also modelled in the TPS by modifying the actual fluence. In MLC-defined fields, the lateral sides of some leaves effectively limit the beam and the exposed tongues from those leaves modify the delivered fluence by blocking some additional radiation. This effect is modelled by extending the leaf projection in the direction perpendicular to the leaf motion by a certain tongue width; thus, the tongue width is subtracted from the delivered fluence (Varian Medical Systems; 2014). This parameter is not configurable in ECLIPSE and is set to 0.3125 mm, slightly smaller than the real tongue width (Torsti et al.; 2013). The groove also modifies the fluence, but that effect is much smaller and is not modelled in the TPS. As a consequence, the field size in the direction of leaf movements is enlarged by the dosimetric leaf gap, while in the perpendicular direction it is reduced due to the tongue width by 0.625 mm (0.3125 mm for each limiting leaf side).

Configuration of calculation algorithms in ECLIPSE also includes the parameters effective spot size (ESS) in the X and Y directions of the collimator coordinate system. These parameters modify the calculated penumbra by applying a Gaussian smoothing to the energy fluence of primary photons (Varian Medical Systems; 2014). In consequence, manual tuning of the ESS in the X and Y direction can be used to adjust the output factor for small MLC apertures and the penumbra width (Fogliata et al.; 2016). For the AAA algorithm and MLC-shaped beams from Varian treatment units, the recommended ESS values are 1 mm and 0 mm for X and Y directions, respectively. However, the ESS in the Y-direction (the direction of the tongue width) was considered potentially relevant and was investigated in the present study. To this aim, calculations were also carried out with the AAA algorithm setting the ESS in the Y direction to 0.5 mm and 1 mm.

3. Results

3.1. Static fields

The results obtained for the combination of the two static fields with complementary MLCs are shown in figure 1, where measured and calculated inplane profiles (along the y axis) are given. Profiles measured with film clearly show the underdosage produced by the TG effect in the interleaf regions. For both MLC models this underdosage is more pronounced in the central part of the field. This can be explained because the central leaves are thinner than the outer leaves, hence increasing the number of dose dips and therefore the overall TG effect. As already described by Deng et al. (2001) and Kim et al. (2015) as depth increases the dose profile is smoothed, with more rounded and

wider dose dips due to electron transport.
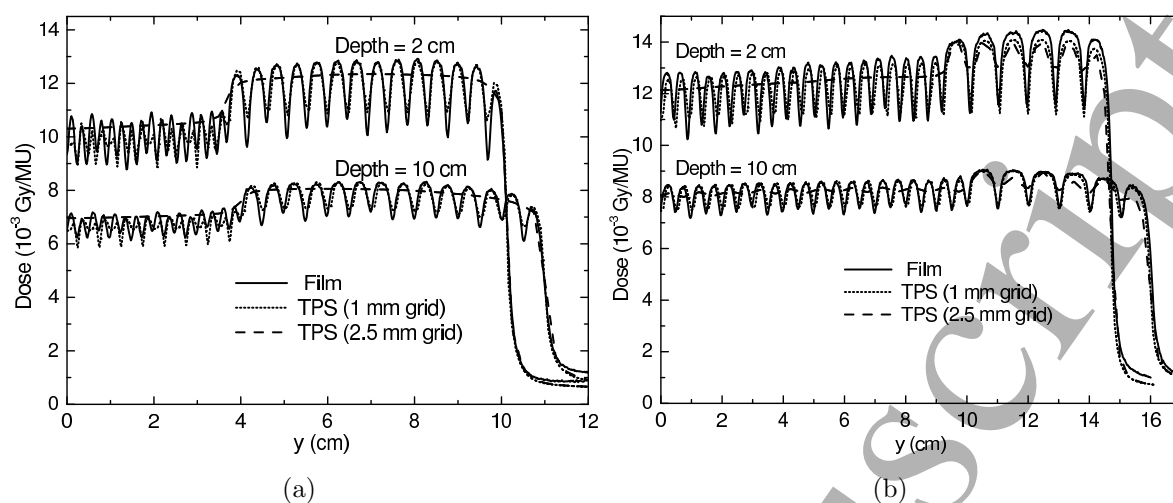
Figure 1. Experimental and calculated profiles obtained for the static test with (a) HDMLC and (b) Millennium MLC.

TPS calculations with the 1 mm grid show good agreement with film dosimetry, indicating that the TPS accurately models the TG effect in this situation regardless of the depth. TPS calculations with the 1 mm grid reproduce the dose profile measured with film in detail, although a finer resolution would be necessary to accurately sample the thinner leaves of the HDMLC (Yang et al., 2016). On the contrary, TPS calculations with the 2.5 mm grid cannot replicate the variations produced by the TG effect in any of the cases evaluated, because this resolution is excessively low.

Measurements with the Farmer ionisation chamber were also carried out at the centre of the beam and compared to film doses and TPS calculations. To verify that the chamber provided a good estimate of the average dose, measurements were repeated for different chamber positions. Thus, positioning shifts between 1 mm and 5 mm were evaluated for both lateral and longitudinal directions. In all cases results were within $\pm 0.2\%$ regardless of the chamber position. Average doses from film were computed by averaging over a $2 \times 2 \, \text{cm}^2$ region. Good agreement was found between film dosimetry and the ionisation chamber measurements, with deviations $< 1\%$, which validates the followed procedure.

To compute the average calculated dose, a cylindrical structure simulating the Farmer chamber was defined in the TPS (diameter = 6 mm, length = 22.5 mm) and the mean dose to the structure was obtained. In general, a good agreement was found between average calculated and measured doses except for the central leaves of the HDMLC. For these leaves, average doses calculated with the 2.5 mm grid were 5.5% higher than those obtained with the 1 mm grid. In particular, the TPS underestimated the average dose with respect to measurements by 1.5% for the 1 mm grid and overestimated it by 4.0% for the 2.5 mm grid. For the the outer leaves of the HDMLC the difference between average doses calculated with both grids was about 2%

Commissioning of the tongue-and-groove modelling in TPS   11

and for all the leaves of the Millennium MLC differences were <1%.

Since the position of the calculation grid could also have an impact on the calculated doses, TPS calculations were repeated at slightly different positions of the calculation grid. No differences in the calculated dose were found for the 2.5 mm grid. For the 1 mm grid dose differences as high as 5% were found at some points near steep dose gradients; however, average doses obtained as mean doses to the cylindrical structure were practically not affected by the position of the calculation grid, with deviations <0.2%.

3.2. Sliding window beams

Figure 2 shows the profiles obtained with film dosimetry for the sweeping gaps of 5 mm and 10 mm at 10 cm depth for different TG fractions, together with the profiles calculated by the TPS for both the HDMLC and the Millennium models.

In absence of tongue-and-groove –figures 2(a) and 2(b)– good agreement between measurements and calculations was found. Film dosimetry profiles show a pattern of alternate peak and valley doses due to the higher interleaf transmission, while calculated profiles are flat because the TPS only takes into account the average transmission. This effect is more evident for smaller gaps because the smaller the gap, the lower the Gy/MU and the higher the contribution of MLC transmission. It can also be seen that the measured profile is slightly lower for the outer leaves than for the inner leaves. This difference can be explained by the off-axis reduction of transmission (Lorenz et al.; 2007) and the lower average transmission of the outer leaves. In this case, no difference was found between the profiles calculated with grids of 1 mm and 2.5 mm.

For half the gap with tongue-and-groove (TG fraction = 0.5, see figures 2(c) and 2(d)), average doses were reduced by the TG effect, especially in the central part of the beam, where the leaves are thinner and therefore the incidence of the TG effect is higher. For small gaps the peak-to-valley variations are low because the TG effect and the interleaf transmission tend to cancel out (LoSasso et al.; 1998). Indeed, the TG decreases the dose between leaves, while interleaf transmission has the opposite effect. The TPS underestimates the dose for the inner leaves, especially when the 1 mm calculation grid is used. Interestingly, for the sweeping gap of 5 mm with the Millennium MLC (and also for the outer leaves of the HDMLC) the film profile shows a pattern of peak-to-valley doses opposite to that calculated by the TPS. The reason for this behaviour is that in this case the interleaf transmission actually dominates over the TG effect, but it is not properly accounted for by the TPS.

Figures 2(e) and 2(f) show the profiles for the situation where the full gap suffers from TG effect (TG fraction = 1), that is, when the separation between adjacent leaves equals the size of the gap. In this case both the reduction in the average dose and the peak-to-valley variations are more pronounced due to the higher TG effect. Similarly to TG fraction = 0.5, TPS calculations clearly underestimate the dose in the central part of the beam, remarkably for the 1 mm grid.

Commissioning of the tongue-and-groove modelling in TPS   12
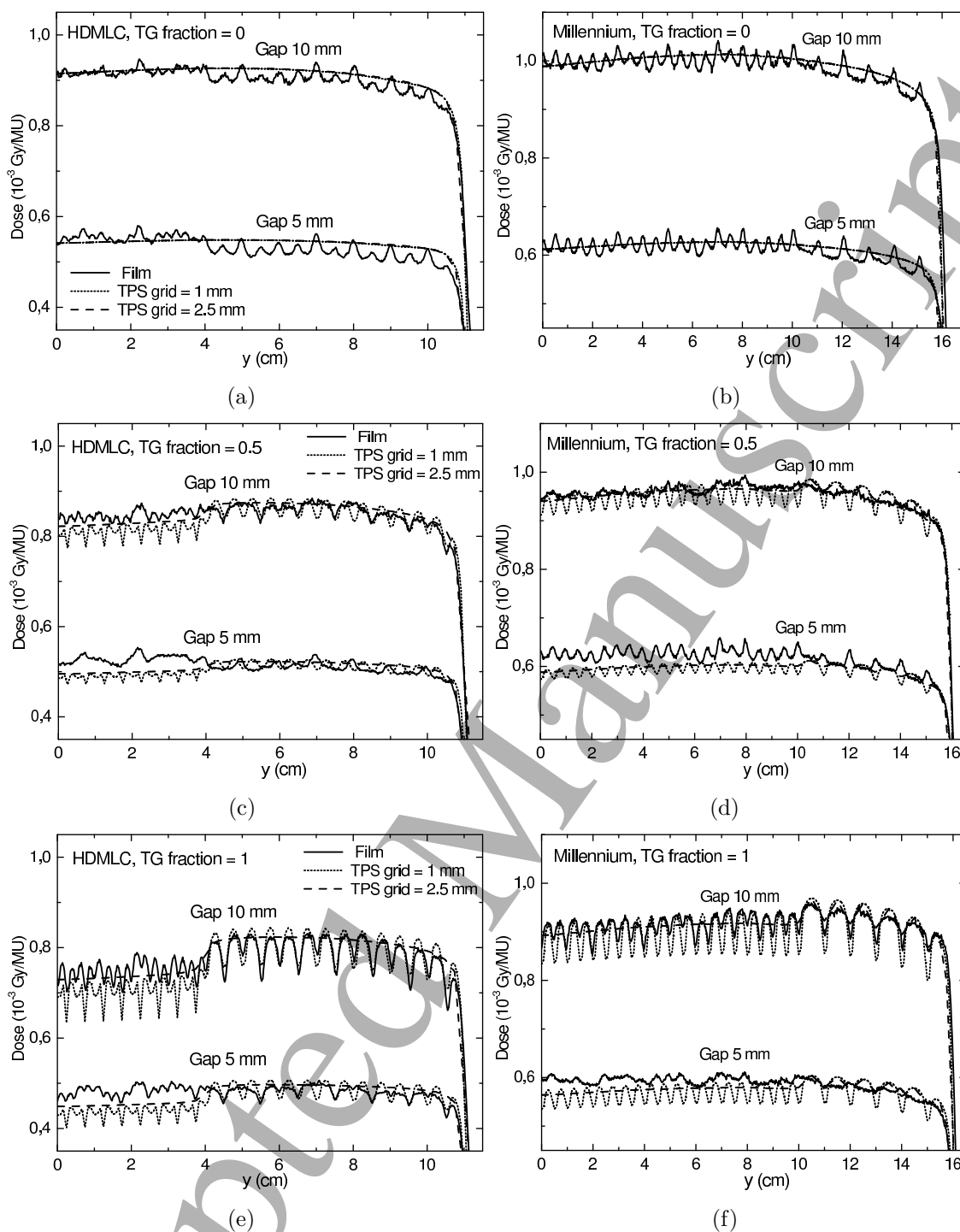
Figure 2. Experimental and calculated profiles obtained for the a-SG test for dynamic gaps of 5 mm and 10 mm at 10 cm depth. Results for the HDMLC (a,c,e) and the Millennium MLC (b,d,f) are shown as a function of the TG fraction.

Figure 3 shows the results for the sweeping gap of 20 mm at 10 cm depth. As expected, the peak-to-valley dose variations are larger than those found for the gaps of 5 mm and 10 mm, because the larger the gap, the lower the contribution of the

MLC transmission and the more evident the TG effect. Having different TG fractions included in the same figure clearly illustrates the average dose reduction introduced by the TG effect. For the HDMLC model this reduction was about 10% (TG = 0.5) and 23% (TG = 1), irrespective of the depth. For the Millennium model the average dose reduction was lower, about 5% for TG = 0.5 and 11% for TG = 1, because the leaves are twice as wide and therefore the TG effect is approximately halved. The TPS is able to approximately reproduce the dose reduction due to the TG effect. However, it tends to overestimate this dose reduction, especially for the thinner leaves and for the 1 mm calculation grid.
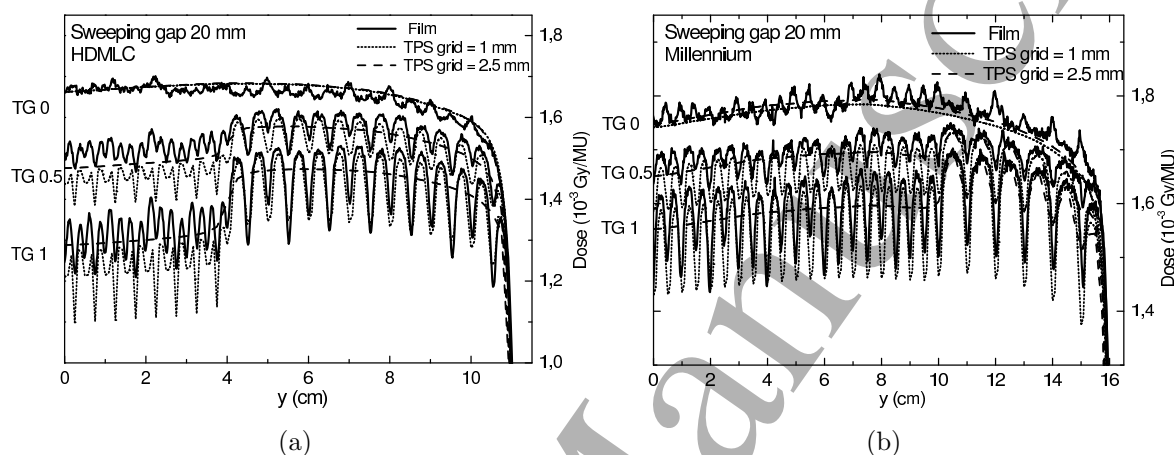
Figure 3. Experimental and calculated profiles obtained for the a-SG test with the (a) HDMLC and (b) Millennium MLC. Results for the dynamic gap of 20 mm at a depth of 10 cm are shown for TG fractions of 0, 0.5 and 1.

Film dosimetry measurements and calculations were also performed at a depth of 2 cm. The peak-to-valley variations produced by the TG effect were smoothed with depth due to scatter and electron transport. Curves are not shown, but the behaviour was very similar to the static case illustrated in figure 1. Profiles were also measured and calculated at off-axis distances, but no differences were found. Tests were also carried out for MLC gaps sweeping a shorter distance (from -3 cm to $+3$ cm) and only slight differences were observed, associated to the smaller effect of the MLC transmission.

Finally, measurements were also performed with a Farmer ionisation chamber in order to determine the mean dose in the central part of the beam. The sensitive volume of this chamber should average the peaks and valleys produced by the TG effect and provide a good estimate of the mean dose. This was experimentally verified by repeating measurements after introducing longitudinal shifts in the chamber position (range 1-5 mm with 1 mm step) and variations in the chamber readings were $<0.2\%$.

Average calculated doses were, again, obtained as the mean dose in the cylindrical structure simulating the chamber. Figures 4(a) and 4(b) show the measured and calculated average doses for the a-SG test. The MLC gap sizes studied were 5, 10, 20 and 30 mm, and for each gap size several TG fractions were evaluated. As the TG fraction

Commissioning of the tongue-and-groove modelling in TPS   14

was increased, the average dose was progressively decreased, until full TG was achieved. The maximum TG effect occurred for TG fractions slightly over 1, due to the influence of the rounded leaf ends. TPS calculations approximately reproduced the dose reduction due to the TG effect, but some discrepancies appeared. For TG fraction $= 0$ a very good agreement was found, with differences $< 0.5\%$. This was expected because the dosimetric leaf gap was measured and the TPS was commissioned precisely in these conditions (without the TG effect). However, as the TG fraction increased, TPS calculations progressively underestimated the dose, notably for the 1 mm grid size. This trend was reversed for TG fractions > 1, where calculated doses remained constant while measured doses kept slightly decreasing.
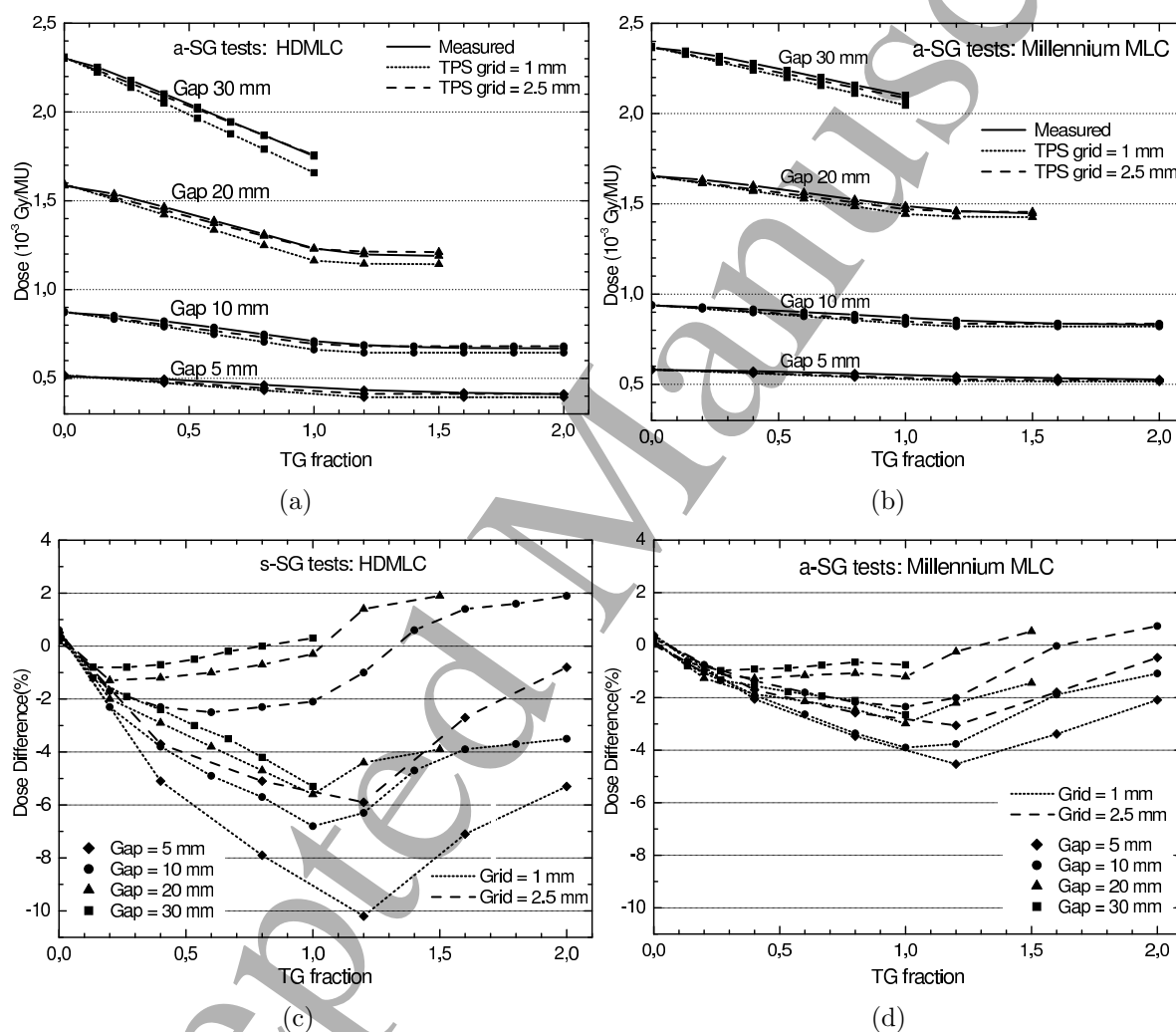
Figure 4. Experimental and calculated average doses for the a-SG test for dynamic gaps of 5, 10, 20 and 30 mm. Results for the (a) HDMLC and the (b) Millennium MLC are given as a function of the TG fraction. Difference between calculations and experiments are given for the (c) HDMLC and the (d) Millennium MLC.

Dose differences given in figures 4(c) and 4(d) clearly illustrate the tendency of the TPS to underestimate the average dose. In general, dose differences do not show a

Commissioning of the tongue-and-groove modelling in TPS   15

linear trend: they progressively increase as the TG fraction augments from zero to one and are gradually reduced for TG fractions greater than one (i.e., when intergitation between leaves from opposed banks occurs). Dose discrepancies for the HDMLC are approximately a factor 2 larger than those found for the Millennium MLC. This can be explained because the incidence of the TG effect is higher for the HDMLC and limitations in the TPS modelling will also have a greater effect. The MLC gap size and the calculation grid also have a great impact on dose discrepancies. Indeed, deviations for the 1 mm grid are much larger than those obtained for the 2.5 mm grid and the smaller the MLC gap, the larger the dose differences. Remarkably, the most adverse combination was the HDMLC with a 5 mm gap calculated with a 1 mm grid, which produced a dose difference as high as 10% .

The potential impact of the effective spot size (ESS) parameter in the Y direction was investigated. Increasing the parameter from 0 to 1 mm produced a progressive smoothing of the dose distribution in that direction. Thus, peak-to-valley variations in dose profiles along the Y direction were reduced by up to 50% when the ESS was increased from 0 to 1 mm. We found that the dose profiles measured with film dosimetry were reproduced much better by the TPS with ESS = 0 mm in the Y direction, which agrees with the manufacturer's recommendation. However, modifying the ESS parameter had no impact on the average doses, with all differences <0.1%. Therefore, the dose discrepancies shown in figures 4(c) and 4(d) remained unaltered. This was expected, because the spot size has a blurring effect on the primary fluence but should not alter average doses.

3.3. VMAT arcs

The a-OSG tests described in section II.B.3 were carried out for the MLC gaps of 10, 20 and 30 mm and for several TG fractions. Figure 5 shows the calculated dose distribution obtained for the HDMLC, 20 mm gap and TG fraction = 1 together with the corresponding dose distribution measured with film. This test produced very homogeneous dose distributions, even in the presence of TG effect. Indeed, film dosimetry showed dose variations around ±2% and measurements with the ionisation chamber placed in different positions revealed differences in average doses within ±0.4%. In the presence of the TG effect TPS calculations show a certain granularity in the dose distribution that might be interpreted as calculation artifacts produced by the limited angular resolution or by the finite grid size. However, this is not the case because film dosimetry also reveals the same effect, showing that the granularity is actually produced by the TG effect, which does not completely smear out during the gantry rotation.

It can also be observed in figures 5(a) and 5(c) that the dose distribution along the gantry rotation axis is slightly less homogeneous than at the rest of the central homogeneous region sketched in figures 5(a) and 5(b). This is because in this axis the projection of the leaf edges coincides at the same points regardless of the gantry angle and the TG effect and interleaf transmission do not smear out during the gantry

Commissioning of the tongue-and-groove modelling in TPS   16

rotation. For this reason we analysed the profiles along a line shifted 5 mm in the x direction, as indicated in figure 5(c).
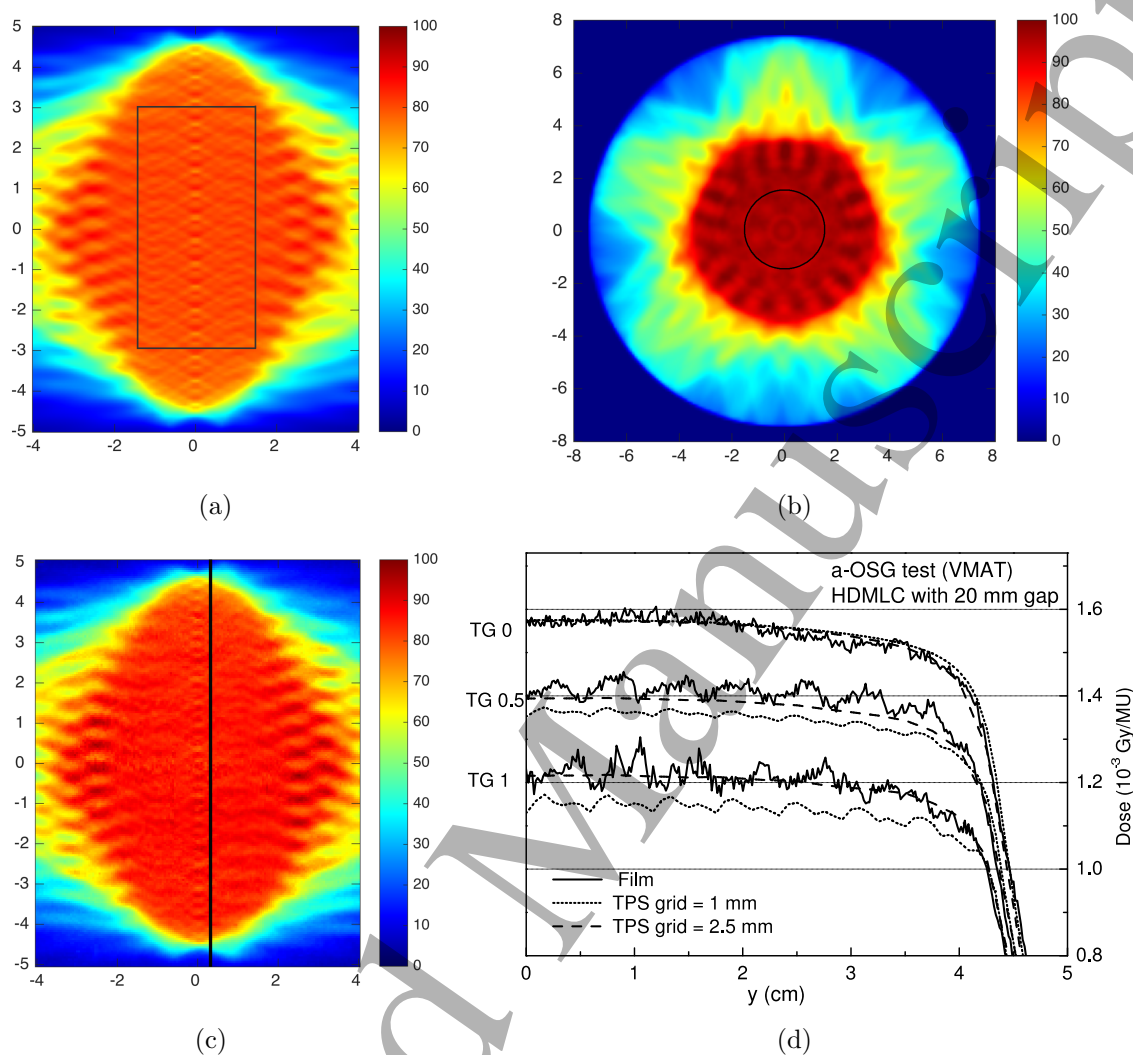

Figure 5. Dose distributions for the a-OSG test with the HDMLC and the 20 mm gap. The calculated distribution at the isocentre level for TG fraction = 1 is illustrated in the (a) horizontal plane and (b) axial plane. The distribution measured with film dosimetry is shown in (c). In (d) dose profiles along the straight line depicted in (c) are given for TG fractions 0, 0.5 and 1. The central region of the quasi-uniform dose region is shown in (a) with a rectangle 6 cm high and 3 cm wide and in (b) with a circle of diameter of 3 cm.

Plans were calculated at gantry angle intervals of approximately 2 deg, which is the configuration used in clinical practice. To evaluate the potential effect of limited angular resolution, some calculations were also carried out every 1 deg, but no relevant differences were observed.

Measurements were also performed with the Farmer ionisation chamber placed in the centre of the cylindrical phantom. As shown in figure 6, good agreement was found for the average doses in the absence of TG the effect (TG = 0), while dose discrepancies

Commissioning of the tongue-and-groove modelling in TPS　　　　　　17

progressively increased as the TG fraction was raised. Similarly to the results from the sweeping gap tests, discrepancies were larger for the HDMLC, small gaps and the 1 mm grid. For the combination of HDMLC, 10 mm gap (which was the smallest gap evaluated for VMAT) and 1 mm grid, the TPS was found to underestimate the dose by 7.4%. This discrepancy is compatible with the result of −6.8% obtained for the same combination with the a-SG test.
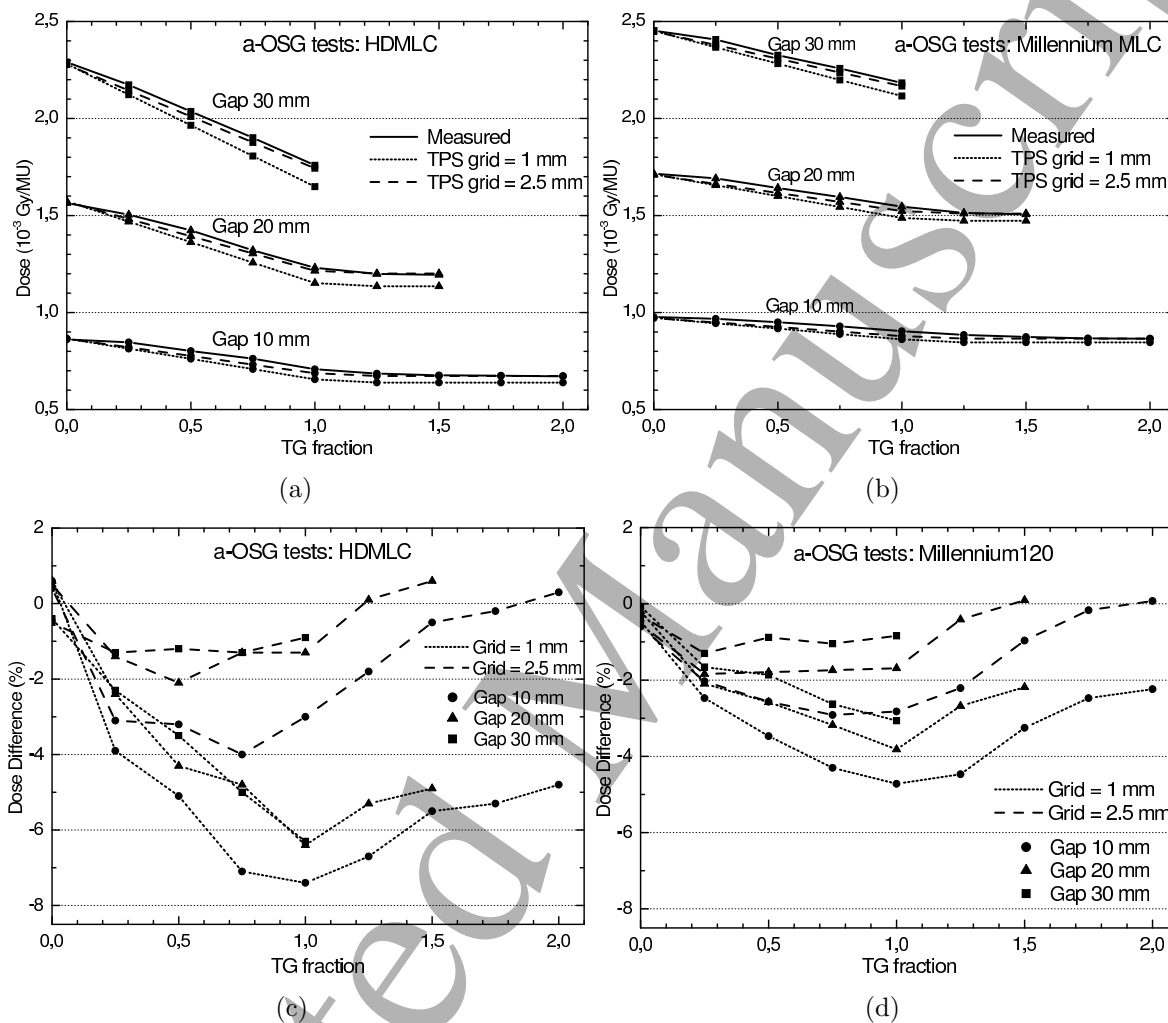
Figure 6. Experimental and calculated average doses for the a-OSG test for gaps of 10, 20 and 30 mm. Results for the (a) HDMLC and the (b) Millennium MLC are given as a function of the TG fraction. Difference between calculations and experiments for the HDMLC and the Millennium MLC are given in (c) and (d), respectively.

The cylindrical PMMA phantom was used in order to take advantage of the cylindrical symmetry of the a-OSG test about the gantry rotation axis and achieve a quasi-uniform dose distribution. However, measurements were repeated with the EASY CUBE phantom and the homogeneity of the dose distribution at the center region remained practically unaltered. As a consequence, other phantoms, not necessarily cylindrical, can be used for the a-OSG tests.

Commissioning of the tongue-and-groove modelling in TPS 18

For comparison purposes, VMAT calculations were also carried out with the AcurosXB algorithm implemented in ECLIPSE. After renormalising to the corresponding 10 x 10 cm2 field, discrepancies between the algorithms AcurosXB (for both dose to water and dose to medium) and AAA disappeared, with differences <0.3%. As a consequence, the dose differences obtained for the AAA algorithm as a function of the TG fraction are also valid for the AcurosXB algorithm.

3.4. Other centres

To verify that similar results could be reproduced with other implementations of the ECLIPSE TPS and different beam data the proposed tests were also carried out in additional linacs from other institutions (table 1). Thus, the following systems were evaluated: (a) TrueBeam STx equipped with an HDMLC and ECLIPSE v11.0 and v13.7 and (b) Clinac 2100CD with a Millennium MLC and ECLIPSE v10.0. The results obtained for the a-SG tests are given in figure 7. Dose differences corresponding to the a-OSG tests were also similar to those from the a-SG tests and so are not shown.
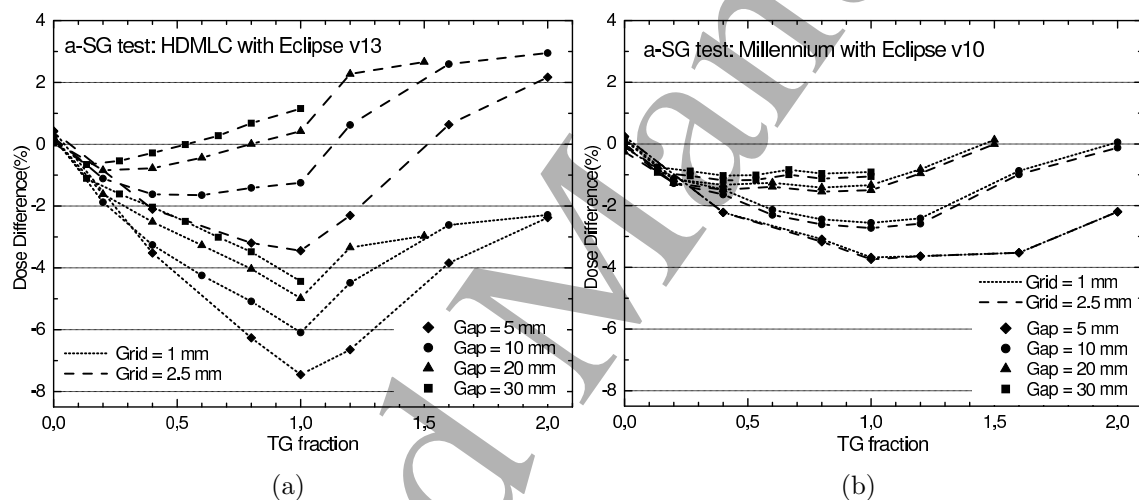
Figure 7. Experimental and calculated average doses for the a-SG test for gaps of 5, 10, 20 and 30 mm. Differences between calculations and experiments corresponding to the a-SG test are given as a function of the TG fraction for (a) HDMLC and Eclipse v13 (centre B) and (b) Millennium MLC and Eclipse v10 (centre C)

Dose differences for the TrueBeam system with an HDMLC and Eclipse v13.7, illustrated in figure 7(a), were similar to those found for the same MLC and ECLIPSE v13.5. Again, results greatly differed depending on the size of the calculation grid, with much larger discrepancies between calculations and measurements for the 1 mm grid. In this case, differences in average doses as high as −7.5% and −6.1% were found for the 5 mm and the 10 mm gaps, respectively. Only data from ECLIPSE v13.7 is shown because version 11.0 produced practically the same results.

The Clinac 2100CD with a Millennium MLC and ECLIPSE v10, on the contrary, behaved differently from the same MLC and ECLIPSE v13 (see figures 7(b) and 4(d)).

Indeed, with ECLIPSE v10 only slight differences around 0.2% were found between the calculation grids of 1 mm and 2.5 mm. Dose discrepancies between calculations and measurements with version 10 were in between those found for the two grid sizes with ECLIPSE v13, with maximum differences of 3.7% and 2.7% for the 5 mm and the 10 mm gaps, respectively.

4. Discussion

4.1. Proposed tests and TPS commissioning

We have demonstrated that, in order to properly calculate the dose patterns produced by the TG effect, TPSs should incorporate modelling of the interleaf transmission. However, since the TG effect from multiple beams (or arcs) tends to smear out, the most relevant quantity is the average dose.

All the proposed tests are suitable for measurements with ionisation chambers or film dosimetry. Film dosimetry provides detailed information about the spatial distribution of dose deposition, which is crucial to properly characterise the TG effect due to its geometric and spatially distributed nature. Additionally, ionisation chambers with a large active volume are recommended for obtaining the average dose delivered by several leaves, which is the most important quantity in clinical treatments. Thus, one of the relevant results of this study is that an ionisation chamber can be used not only for measuring the dosimetric leaf gap and the MLC transmission, but also for evaluating the TPS modelling of the TG effect. Actually, using a chamber with a large sensitive volume (such as a Farmer-type chamber) is even beneficial because it spatially averages small dose inhomogeneities, providing a robust determination of the mean dose.

The tests proposed in this study allow evaluation of the TPS modelling of the tongue-and-groove. Hence, they can be used for the commissioning of TPSs and also for the validation of TPS upgrades, although there is no consensus on the acceptance level that should be used. Recent Practice Guidelines from AAPM (Smilowitz et al.; 2015) recommend that average differences between TPS and measurements with ionisation chambers should not exceed 2% in low-gradient target regions produced by IMRT treatments. Our results show that these recommendations may not be fulfilled, even in quasi-homogeneous dose distributions, due to limitations in the modelling of the TG effect in the TPS. Thus, agreement within ±2% would be desirable but, to this aim, improved modelling of the MLC is necessary.

It is worth highlighting that, although we focused on the Varian solution (ECLIPSE TPS and Varian linacs), the tests proposed can be applied to any TPS and linac combination. In particular, in TPSs where the value of the tongue-and-groove width can be configured (Chen et al.; 2015), these tests can also be used to obtain the optimal value for this parameter.

Commissioning of the tongue-and-groove modelling in TPS 20

4.2. Results

For the static test, as already reported by Van Esch et al. (2011), TPS calculations with the 1 mm grid agreed well with measurements and were capable of reproducing the pattern of dose dips and peaks. This test is independent of the leaf gap setting, but it reflects a situation of static MLC with maximum leaf aperture and maximum TG effect that it is not representative of the fields used in clinical practice.

On the contrary, the a-SG and a-OSG tests evaluate dynamic MLCs and cover a wide range of MLC gap sizes and TG fractions similar to those used in clinical treatments. In the presence of the TG effect both film dosimetry and ionisation chambers, which agreed to within 1%, exposed some relevant dose differences between calculations and measurements, especially for the inner leaves. The fact that differences between calculations and measurements did not show a linear trend indicates inadequate modelling of the tongue-and-groove rather than only a non-optimal setting of the tongue width within the TPS. Indeed, any change in the tongue width would, in principle, produce a change in the slope of the calculated curves shown in figures $4(a), 4(b), 6(a)$ and $6(b)$. This parameter is not user-configurable in ECLIPSE, but such a change would not completely eliminate the discrepancies obtained.

In general, we found that the smaller the MLC gap, the larger the dose difference. A possible explanation is that limitations of the tongue-and-groove modelling in the TPS originate a certain error in the calculated fluence that will have a higher relative impact on small gaps. These differences can provide insight into dosimetric discrepancies related to the use of small MLC gaps in dynamic treatments (Fog et al.; 2011; Kielar et al.; 2012).

It was surprising to find differences of up to 5% between average doses calculated with different grid sizes with both ECLIPSE v11 and v13, even in the homogeneous dose distributions produced by the a-OSG tests. It is known that changing the grid size may affect the calculated dose, especially for small fields, small MLC apertures and in regions with high dose gradients (Ong et al.; 2011). However, the mean and the integral dose (i.e., the total energy deposited) should not depend on the grid size (Torsti et al.; 2013). In the absence of the TG effect, calculations for the a-OSG tests with both grid sizes agreed, while discrepancies increased as the TG fraction increased. This clearly indicates a problem in the TPS that could be overlooked without these tests. Investigating the exact cause of these differences is beyond the scope of this study. However, it has been seen that grid alignment can cause sampling errors that could affect the calculated dose (Yang et al.; 2016). Differences might also be associated to the unified fluence calculation implemented in version 11 of ECLIPSE, which would explain why in ECLIPSE v10 calculations with both grid sizes agreed to within $\pm 20.2\%$ in all cases (figure 7(b)).

The results for AcurosXB were practically identical to those obtained for the AAA, with average dose differences lower than 0.3%. Accuracy of ECLIPSE TPS calculations is affected by both the source model –that includes the modelling of the MLC– and the

Commissioning of the tongue-and-groove modelling in TPS 21

dose deposition algorithm, which is responsible for radiation transport and conversion to absorbed dose. Our results indicate that, although their dose deposition engine is totally different, both algorithms use the same MLC modelling and suffer from the same limitations regarding the TG effect.

Two additional centres carried out the tests and obtained similar results, which would rule out the possibility of problems related to a particular implementation or configuration of the TPS.

4.3. Clinical implications and considerations

In the present study we have reported some important discrepancies between calculations and measurements that can clearly yield clinical consequences in certain situations. Although in clinical plans with dynamic MLCs the TG effect is spatially smeared out, the average dose is underestimated by the TPS, as we confirmed with the a-OSG tests. However, the ECLIPSE TPS has been thoroughly validated and it is well established that it offers satisfactory dose calculations for IMRT/VMAT treatments, including SBRT treatments (Gagne et al.; 2008; Fogliata et al.; 2011). Recently it has also been shown that ECLIPSE offered acceptable characteristics for stereotactic small fields provided adequate tuning of configuration parameters is performed (Fogliata et al.; 2016).

The apparent discrepancy between our results and those reported in the literature can be explained in two ways. Firstly, clinical plans involve continuous distributions of MLC gaps and TG fractions; therefore, the dose differences found in the proposed tests will be averaged and might partially cancel each other out. Secondly, configuration parameters in TPSs are often tuned in order to maximise agreement between measurements and calculations in clinical plans, which might mask the problem. Indeed, systematic differences introduced by inadequate MLC modelling in the TPS may be partially compensated by tuning parameters in the TPS, providing better agreement between calculations and measurements for typical clinical plans. For instance, incrementing the dosimetric leaf gap will increase the doses calculated by the TPS and the smaller the MLC gap, the higher the dose increase. Hence, tuning the dosimetric leaf gap can be a rather effective method to compensate for the underestimation of the calculated doses produced by inadequate modelling of the TG effect.

Kielar et al. (2012) reported the need to tune the dosimetric leaf gap parameter in the ECLIPSE TPS for dynamic treatments involving small MLC gaps, especially for the HDMLC, although the reasons were not identified. Our study supports their results and explains the need for tuning configuration parameters in the TPS. However, these parameters will not be optimal for all plans and compensations might not work in certain cases (Yao and Farr; 2015). In our opinion, improving the MLC modelling will both increase the accuracy of the TPS and reduce the need for tuning configuration parameters.

Our study reveals some limitations in the tongue-and-groove modelling within the

REFERENCES　　　　　　　　　　　　　　　　　　　　　　　22

ECLIPSE TPS and raises concerns about the accuracy of calculations with the 1 mm grid in certain situations, but it does not invalidate the clinical applicability of the TPS. Some investigators have reported improved accuracy for calculations with ECLIPSE when the finer 1 mm grid is used (Ong et al.; 2011). Again, this work does not conflict with that, because our study focused on the TG effect, and overall accuracy in clinical plans was not addressed. Nevertheless, the combination involving the HDMLC and the 1 mm grid is typically used for small target volumes and plans with high complexities, which are also associated to small MLC gaps (Fog et al.; 2011). Since this was the combination yielding the largest discrepancies, we believe that in these cases the limitations reported in the present study are especially relevant and should be carefully evaluated.

5. Conclusions

In this study we have characterised the dosimetric consequences of the tongue-and-groove effect and we have presented comprehensive tests to evaluate the ability of TPSs to accurately model this effect. The tests proposed can be useful for the commissioning of TPSs and for the validation of major upgrades. Relevant differences between calculations and measurements for beams with dynamic MLCs in the presence of the TG effect were found for the ECLIPSE TPS, especially for the HD120 MLC, small gap sizes and the 1 mm calculation grid.

In conclusion, there is a need for better modelling of the MLC by TPSs, and one of the relevant aspects is the tongue-and-groove. In our opinion, this will improve the accuracy of TPS calculations, particularly for highly modulated plans or those with small target volumes, which involve small MLC gaps and are especially challenging to calculate. In addition, improved modelling of the MLC would greatly reduce the need for tuning parameters in the TPS, facilitating a more comprehensive configuration and commissioning of TPSs.

References

Bhagwat, M. S., Han, Z., Ng, S. K. and Zygmanski, P. (2010). An oscillating sweeping gap test for VMAT quality assurance., *Physics in Medicine and Biology* **55**(17): 5029–5044.

Chen, S., Yi, B. Y., Yang, X., Xu, H., Prado, K. L. and D'Souza, W. D. (2015). Optimizing the MLC model parameters for IMRT in the RayStation treatment planning system, *Journal of Applied Clinical Medical Physics* **16**(5): 322–332.

Deng, J., Pawlicki, T., Chen, Y., Li, J., Jiang, S. B. and Ma, C. M. (2001). The MLC tongue-and-groove effect on IMRT dose distributions., *Physics in Medicine and Biology* **46**(4): 1039–60.

Fix, M. K., Volken, W., Frei, D., Frauchiger, D., Born, E. J. and Manser, P. (2011). Monte Carlo implementation, validation, and characterization of a 120 leaf MLC., *Medical physics* **38**(10): 5311–20.

REFERENCES   23

Fog, L. S., Rasmussen, J. F. B., Aznar, M., Kjær-Kristoffersen, F., Vogelius, I. R., Engelholm, S. A. and Bangsgaard, J. P. (2011). A closer look at RapidArc® radiosurgery plans using very small fields., *Physics in Medicine and Biology* **56**(6): 1853–1863.

Fogliata, A., Lobefalo, F., Reggiori, G., Stravato, A., Tomatis, S., Scorsetti, M. and Cozzi, L. (2016). Evaluation of the dose calculation accuracy for small fields defined by jaw or MLC for AAA and Acuros XB algorithms, *Medical Physics* **43**(10): 5685–5694.

Fogliata, A., Nicolini, G., Clivio, A., Vanetti, E. and Cozzi, L. (2011). Accuracy of Acuros XB and AAA dose calculation for small fields with reference to RapidArc® stereotactic treatments Accuracy of Acuros XB and AAA dose calculation for small fields with reference to RapidArc V R stereotactic treatments, *Medical Physics* **38**(38): 31714–3666.

Gagne, I. M., Ansbacher, W., Zavgorodni, S., Popescu, C. and Beckham, W. a. (2008). A Monte Carlo evaluation of RapidArc dose calculations for oropharynx radiotherapy., *Physics in Medicine and Biology* **53**(24): 7167–7185.

IAEA (2007). Specification and Acceptance Testing of Radiotherapy Treatment Planning Systems. TECDCOC 1540, *IAEA TECDOC* (April).

IAEA (2008). Commissioning of Radiotherapy Treatment Planning Systems : Testing for Typical External Beam Treatment Techniques Commissioning of Radiotherapy Treatment Planning Systems : Testing for Typical External Beam Treatment Techniques. TECDOC 1583, *IAEA TECDOC* (January).

Kielar, K. N., Mok, E., Hsu, A., Wang, L. and Luxton, G. (2012). Verification of dosimetric accuracy on the TrueBeam STx: rounded leaf effect of the high definition MLC., *Medical Physics* **39**(10): 6360–71.

Kim, H. J., Kim, S., Park, Y. K., Kim, J. I., Park, J. M. and Ye, S. J. (2015). Multileaf collimator tongue-and-groove effect on depth and off-axis doses: A comparison of treatment planning data with measurements and Monte Carlo calculations, *Medical Dosimetry* **40**(4): 271–278.

Lewis, D., Micke, A., Yu, X. and Chan, M. F. (2012). An efficient protocol for radiochromic film dosimetry combining calibration and measurement in a single scan, *Medical Physics* **39**(10): 6339–6350.

Li, J. S., Lin, T., Chen, L., Price, R. a. and Ma, C.-M. (2010). Uncertainties in IMRT dosimetry., *Medical physics* **37**(May): 2491–2500.

Lorenz, F., Nalichowski, A., Rosca, F., Killoran, J., Wenz, F. and Zygmanski, P. (2008). An independent dose calculation algorithm for MLC-based radiotherapy including the spatial dependence of MLC transmission., *Physics in medicine and biology* **53**(3): 557–573.

Lorenz, F., Nalichowski, A., Rosca, F., Kung, J., Wenz, F. and Zygmanski, P. (2007).

REFERENCES   24

Spatial dependence of MLC transmission in IMRT delivery., *Physics in Medicine and Biology* **52**(19): 5985–99.

LoSasso, T., Chui, C. and Ling, C. (1998). Physical and dosimetric aspects of a multileaf collimation system used in the dynamic mode for implementing intensity modulated radiotherapy., *Medical physics* **25**(10): 1919–1927.

Mans, A., Schuring, D., Arends, M. P., Vugts, C. A. J. M., Wolthaus, J. W. H., Lotz, H. T., Admiraal, M., Louwe, R. J. W., Öllers, M. C. and van de Kamer, J. B. (2016). The NCS code of practice for the quality assurance and control for volumetric modulated arc therapy., *Physics in Medicine and Biology* **61**(19): 7221–7235.

Mei, X., Nygren, I. and Villarreal-Barajas, J. E. (2011). On the use of the MLC dosimetric leaf gap as a quality control tool for accurate dynamic IMRT delivery., *Medical physics* **38**(4): 2246–2255.

Ong, C. L., Cuijpers, J. P., Senan, S., Slotman, B. J. and Verbakel, W. F. A. R. (2011). Impact of the calculation resolution of AAA for small fields and RapidArc treatment plans., *Medical Physics* **38**(8): 4471–9.

Rosca, F. and Zygmanski, P. (2008). An EPID response calculation algorithm using spatial beam characteristics of primary, head scattered and MLC transmitted radiation., *Medical physics* **35**(6): 2224–2234.

Smilowitz, J. B., Das, I. J., Feygelman, V., Fraass, B. A., Kry, S. F., Marshall, I. R., Mihailidis, D. N., Ouhib, Z., Ritter, T., Snyder, M. G. and Fairobent, L. (2015). AAPM Medical Physics Practice Guideline 5.a.: Commissioning and QA of Treatment Planning Dose Calculations - Megavoltage Photon and Electron Beams, *Journal of Applied Clinical Medical Physics* **16**(5): 14–34.

Torsti, T., Korhonen, L. and Medical, V. (2013). Using Varian Photon Beam Source Model for Dose Calculation of Small Fields, (September).

Van Esch, A., P. Huyskens, D., Behrens, C. F., Samse, E., Sjlin, M., Bjelkengren, U., Sjstrm, D., Clermont, C., Hambach, L., Sergent, F. F. F., Huyskens, D. P., Behrens, C. F., Samsoe, E., Sjolin, M., Bjelkengren, U., Sjostrom, D., Clermont, C., Hambach, L. and Sergent, F. F. F. (2011). Implementing RapidArc into clinical routine: A comprehensive program from machine QA to TPS validation and patient QA, *Medical Physics* **38**(9): 5146.

Varian Medical Systems (2014). Eclipse Photon and Electron Reference Guide, (April): 263–348.

Vera Sanchez, J. A., Ruiz Morales, C. and Gonzalez Lopez, A. (2016). Characterization of noise and digitizer response variability in radiochromic film dosimetry. Impact on treatment verification, *Physica Medica* **32**(9): 1167–1174.

Yang, J., Tang, G., Zhang, P., Hunt, M., Lim, S. B., LoSasso, T. and Mageras, G. (2016). Dose calculation for hypofractionated volumetric-modulated arc therapy: Approximating continuous arc delivery and tongue-and-groove modeling, *Journal of Applied Clinical Medical Physics* **17**(2): 3–13.

REFERENCES   25

Yao, W. and Farr, J. B. (2015). Determining the optimal dosimetric leaf gap setting for
rounded leaf-end multileaf collimator systems by simple test fields, *Journal of applied
clinical medical physics / American College of Medical Physics* **16**(4): 5321.